Quantum chromodynamics in the LHC era

Pavel Nadolsky

Department of Physics
Southern Methodist University (Dallas, TX)

December 9, 2014
Lecture 2

QCD factorization and PDFs

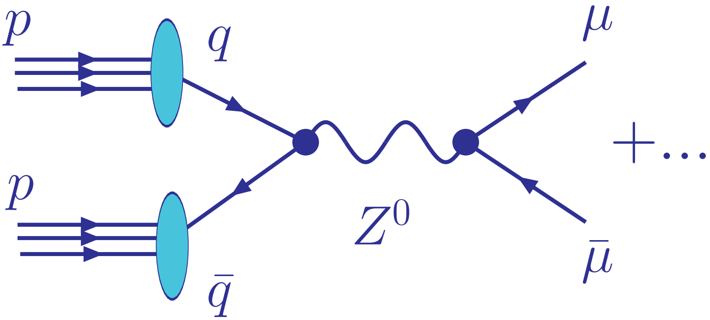

$pp \to (Z^0 \to \mu\bar{\mu})X$: Feynman diagram at the leading order in QCD. Let's now consider higher orders (...).

QCD factorization and PDFs

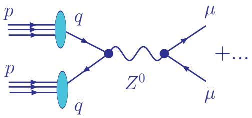

According to QCD factorization theorems, typical cross sections (e.g., for $p(k_1)p(k_2) \to \left[Z(q) \to \ell(k_3)\bar{\ell}(k_4)\right] X$) take the form

$$\sigma_{pp\to\ell\bar{\ell}X} = \sum_{a,b=q,\bar{q},g} \int_0^1 d\xi_1 \int_0^1 d\xi_2\, \widehat{\sigma}_{ab\to Z\to\ell\bar{\ell}} \left(\frac{x_1}{\xi_1}, \frac{x_2}{\xi_2}; \frac{Q}{\mu}\right) f_{a/p}(\xi_1,\mu) f_{b/p}(\xi_2,\mu) + \mathcal{O}\left(\Lambda_{QCD}^2/Q^2\right)$$

- $\widehat{\sigma}_{ab\to Z\to\ell\bar{\ell}}$ is the **hard-scattering cross section**
- $f_{a/p}(\xi,\mu)$ are the **PDFs**
- $Q^2 = (k_3+k_4)^2$, $x_{1,2} = \left(Q/\sqrt{s}\right) e^{\pm y_V}$ — measurable quantities
- ξ_1, ξ_2 are partonic momentum fractions (integrated over)
- μ is a factorization scale (=renormalization scale from now on)

QCD factorization and PDFs

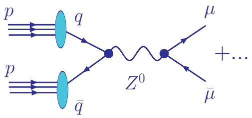

According to QCD factorization theorems, typical cross sections (e.g., for $p(k_1)p(k_2) \to \left[Z(q) \to \ell(k_3)\bar{\ell}(k_4)\right] X$) take the form

$$\sigma_{pp\to\ell\bar{\ell}X} = \sum_{a,b=q,\bar{q},g} \int_0^1 d\xi_1 \int_0^1 d\xi_2\, \widehat{\sigma}_{ab\to Z\to\ell\bar{\ell}} \left(\frac{x_1}{\xi_1}, \frac{x_2}{\xi_2}; \frac{Q}{\mu}\right) f_{a/p}(\xi_1,\mu) f_{b/p}(\xi_2,\mu)$$
$$+ \mathcal{O}\left(\Lambda^2_{QCD}/Q^2\right)$$

- μ is naturally set to be of order Q
- Factorization holds up to terms of order Λ^2_{QCD}/Q^2

QCD factorization and PDFs

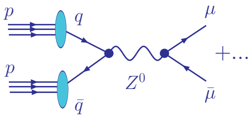

According to QCD factorization theorems, typical cross sections (e.g., for $p(k_1)p(k_2) \to \left[Z(q) \to \ell(k_3)\bar{\ell}(k_4)\right] X$) take the form

$$\sigma_{pp\to\ell\bar{\ell}X} = \sum_{a,b=q,\bar{q},g} \int_0^1 d\xi_1 \int_0^1 d\xi_2\, \widehat{\sigma}_{ab\to Z\to\ell\bar{\ell}}\left(\frac{x_1}{\xi_1}, \frac{x_2}{\xi_2}; \frac{Q}{\mu}\right) f_{a/p}(\xi_1,\mu) f_{b/p}(\xi_2,\mu) + \mathcal{O}\left(\Lambda^2_{QCD}/Q^2\right)$$

Purpose of this arrangement:

- Subtract large collinear logarithms $\alpha_s^n \ln^k(Q^2/m_q^2)$ from $\widehat{\sigma}$
- Resum them in $f_{a/p}(\xi,\mu)$ to all orders of α_s

QCD factorization and PDFs

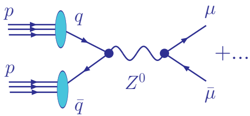

According to QCD factorization theorems, typical cross sections (e.g., for $p(k_1)p(k_2) \to \left[Z(q) \to \ell(k_3)\bar{\ell}(k_4)\right] X$) take the form

$$\sigma_{pp\to\ell\bar{\ell}X} = \sum_{a,b=q,\bar{q},g} \int_0^1 d\xi_1 \int_0^1 d\xi_2 \, \widehat{\sigma}_{ab\to Z\to\ell\bar{\ell}} \left(\frac{x_1}{\xi_1}, \frac{x_2}{\xi_2}; \frac{Q}{\mu}\right) f_{a/p}(\xi_1,\mu) f_{b/p}(\xi_2,\mu)$$
$$+ \mathcal{O}\left(\Lambda^2_{QCD}/Q^2\right)$$

Purpose of this arrangement:

- **Hard** cross sections $\widehat{\sigma}$ depend only on the **partonic** process. They are **computed**.
- **PDFs** $f_{a/h}(\xi,\mu)$ are **universal** functions. They are **defined in QFT and "measured"** for each pair of hadron h and parton a.

Operator definitions for PDFs

To all orders in α_s, PDFs are **defined** as matrix elements of certain correlator functions:

$$f_{q/p}(x,\mu) = \frac{1}{4\pi}\int_{-\infty}^{\infty} dy^- e^{iy^- p^+} \langle p \left| \overline{\psi}_q(0,y^-,\vec{0}_T)\gamma^+\psi_q(0,0,\vec{0}_T) \right| p\rangle, \text{ etc.}$$

Several types of definitions, or **factorization schemes** ($\overline{MS}$, DIS, etc.), exist

They all correspond to the probability density for finding a in p at LO; they differ at NLO and beyond

To prove factorization, one must show that $f_{a/p}(x,\mu)$ correctly captures higher-order contributions for the considered observable

This condition can be violated for multi-scale observables (e.g., DIS or Drell-Yan process at $x \sim Q/\sqrt{s} \ll 1$)

Exercise. Factorization in $pp \to (Z \to e^+e^-)X$

The appendices contain

1. A derivation of the NLO cross section for $pp \to ZX$ **(on-shell Z boson production)** using **cut Feynman diagrams** $|\mathcal{M}|^2$. A lecture by C.-P. Yuan.

2. A derivation of the Born cross section for $pp \to (Z \to e^+e^-)$ (Z boson production and decay) using **helicity amplitudes** $\mathcal{M}_{h_1h_2h_3h_4}$.

Work out these derivations after the lectures.

Derive the LO cross section for a spin-1 boson

Traditional path

Lagrangian$\Rightarrow$Feynman rules $\Rightarrow$
$\sum_{spin} |\mathcal{M}|^2 \Rightarrow \mathrm{Tr}\left(\gamma^{\alpha_1} ... \gamma^{\alpha_n}\right) \Rightarrow$cross section

Helicity amplitudes

Lagrangian$\Rightarrow$"Feynman rules" for helicity amplitudes$\Rightarrow\mathcal{M}\Rightarrow\sum_{spin} |\mathcal{M}|^2 \Rightarrow$ cross section

- Efficient computation of tree diagrams
- are building blocks in unitarity-based QCD calculations

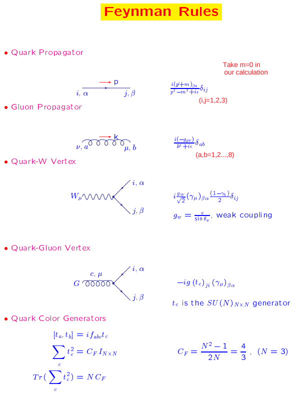

- Many excellent reviews, e.g., *Mangano, Parke, Phys. Rep. 200, 301; Dixon, hep-ph/9601359*

Factorization Theorem

$$\sigma_{hh'} = \Sigma_{i,j} \int_0^1 dx_1 dx_2 \, \phi_{i/h}\left(x, Q^2\right) H_{ij}\left(\frac{Q^2}{x_1 x_2 S}\right) \phi_{j/h'}\left(x_2, Q^2\right)$$

Nonperturbative, but universal, hence, measurable

IRS, Calculable in pQCD

Procedure:

(1) Compute σ_{kl} in pQCD with k, l partons (not h, h' hadron)

$$\sigma_{kl} = \sum_{i,j} \int_0^1 dx_1 dx_2 \, \phi_{i/k}\left(x_1, Q^2\right) H_{ij}\left(\frac{Q^2}{x_1 x_2 S}\right) \phi_{j/l}\left(x_2, Q^2\right)$$

(2) Compute $\phi_{i/k}, \phi_{j/l}$ in pQCD

(3) Extract H_{ij} in pQCD

H_{ij} IRS $\Rightarrow$ H_{ij} indepent of k, l

$\Rightarrow$ same H_{ij} with $(k \to h, l \to h')$

(4) Use H_{ij} in the above equation with $\phi_{i/h}, \phi_{j/h'}$

Extracting H_{ij} in pQCD

- Expansions in α_s:

$$\sigma_{kl} = \sum_{n=0}^{\infty} \left(\frac{\alpha_s}{\pi}\right)^n \sigma_{kl}^{(n)} \qquad \alpha_s = \frac{g^2}{4\pi}$$

$$H_{ij} = \sum_{n=0}^{\infty} \left(\frac{\alpha_s}{\pi}\right)^n H_{ij}^{(n)}$$

$$\phi_{i/k}(x) = \delta_{ik}\delta(1-x) + \sum_{n=1}^{\infty} \left(\frac{\alpha_s}{\pi}\right)^n \phi_{i/k}^{(n)}$$

$\uparrow$ $\phi_{i/k}^{(0)}$ ($\alpha_s = 0 \Rightarrow$ Parton k " stays itself ")

- Consequences:

$$H_{ij}^{(0)} = \sigma_{ij}^{(0)} = \text{“Born”}$$

suppress "^" from now on

$$H_{ij}^{(1)} = \sigma_{ij}^{(1)} - \left[\sigma_{il}^{(0)} \phi_{l/j}^{(1)} + \phi_{k/i}^{(1)} \sigma_{kj}^{(0)} \right]$$

$\sigma_{ij}^{(1)}$, $\sigma_{il}^{(0)}$: Computed from Feynman diagrams (process dependent)

$\phi_{l/j}^{(1)}$, $\phi_{k/i}^{(1)}$: Computed from the definition of perturbative parton distribution function (process independent, scheme dependent)

Feynman Diagrams

- Born level $\alpha_s^{(0)}$ $(q\overline{q'})_{Born}$

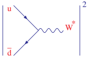

- NLO: $(\alpha_s^{(1)})$ virtual corrections $(q\overline{q'})_{virt}$

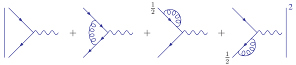

- NLO: $(\alpha_s^{(1)})$ real emission diagrams $(q\overline{q'})_{real}$

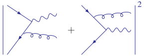

- NLO: $(\alpha_s^{(1)})$ real emission diagrams $(qG)_{real}$

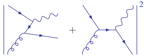

- NLO: $(\alpha_s^{(1)})$ real emission diagrams $(G\overline{q'})_{real}$

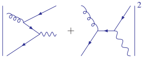

In "Cut-diagram" notation

- $(q\overline{q'})_{Born}$

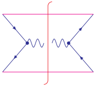

- $(q\overline{q'})_{virt}$

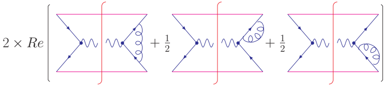

- $(q\overline{q'})_{real}$

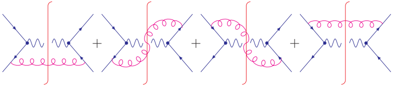

- $(qG)_{real}$

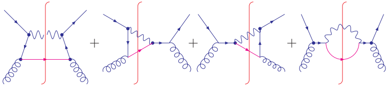

- $(G\overline{q'})_{real}$

  Same as $(qG)_{real}$ after replacing q by $\overline{q'}$.

Immediate problems (Singularities)

- Ultraviolet singularity

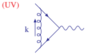

$$\sim \int^{\infty} d^4k \frac{\not{k}\ \not{k}}{(k^2)\,(k^2)\,(k^2)} \rightarrow \infty$$

- Infrared singularities

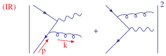

$$\rightarrow \infty$$

as $k^\mu \rightarrow 0$ (soft divergence)

or $k^\mu \parallel p^\mu$ (collinear divergence)

$$\frac{1}{(p-k)^2 - m^2} = \frac{1}{-2p\cdot k} \text{ (for } m = 0 \text{ or } m \neq 0)$$

$p \cdot k \rightarrow 0$ as

$k \rightarrow 0$ or $k^\mu \parallel p^\mu$ (for $m = 0$)

$k \rightarrow 0$ (for $m \neq 0$)

(Similar singularities also exist in virtual diagrams.)

- Solutions

Compute H_{ij} in pQCD in $n = 4 - 2\varepsilon$ dimensions
(dimensional regularization)

(1) $n \neq 4 \Rightarrow$ UV & IR divergences appear as $\frac{1}{\varepsilon}$ poles
in $\sigma_{ij}^{(1)}$ (Feynman diagram calculation)

(2) H_{ij} is IR safe $\Rightarrow$ no $\frac{1}{\varepsilon}$ in H_{ij}
(H_{ij} is UV safe after "renormalization".)

Virtual Corrections $(q\bar{q}')_{virt}$
(in Feynman Gauge)

-  $= 0$

  $\frac{1}{\varepsilon_{IR}}$ and $\frac{1}{\varepsilon_{UV}}$ poles cancel when $\varepsilon_{UV} = -\varepsilon_{IR} \equiv \varepsilon$

- 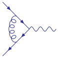

  $\frac{1}{\varepsilon_{UV}}$ cancel $\Rightarrow$ Electroweak coupling is not renormalized by QCD interactions at one-loop order (Ward identity, a renormalizable theory)

  $\frac{1}{\varepsilon_{IR}}$ poles remain

- $\sigma^{(1)}_{virt}$ is free of ultraviolent singularity.

$$\sigma^{(1)}_{virt} = \sigma^{(0)} \frac{\alpha_s}{2\pi} \delta\left(1 - \hat{\tau}\right) \left(\frac{4\pi\mu^2}{M^2}\right)^{\varepsilon} \frac{\Gamma\left(1-\varepsilon\right)}{\Gamma\left(1-2\varepsilon\right)} \cdot \left\{ -\frac{2}{\varepsilon^2} - \frac{3}{\varepsilon} - 8 + \frac{2\pi^2}{3} \right\} \cdot (C_F)$$

$-\frac{2}{\varepsilon^2}$: soft and collinear singularities

$-\frac{3}{\varepsilon}$: soft or collinear singularities

C_F: color factor

$\sigma^{(0)} \equiv \frac{\pi}{12\hat{s}} g_w^2 \cdot (1 - \varepsilon)$

Real Emission Contribution $(q\overline{q}')_{real}$

- 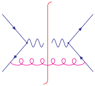

  $\sim \frac{1}{\varepsilon}$ Collinear

  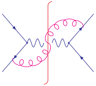

  $\sim \frac{1}{\varepsilon^2}$ Soft and Collinear

-

$$\sigma^{(1)}_{\text{real}}\left(q\overline{q}'\right) = \sigma^{(0)}\frac{\alpha_s}{2\pi}\left(\frac{4\pi\mu^2}{M^2}\right)^{\varepsilon}\frac{\Gamma(1-\varepsilon)}{\Gamma(1-2\varepsilon)}\cdot C_F$$
$$\cdot\left\{\frac{2}{\varepsilon^2}\delta(1-\hat{\tau}) - \frac{2}{\varepsilon}\frac{1+\hat{\tau}^2}{(1-\hat{\tau})_+} + 4\left(1+\hat{\tau}^2\right)\left(\frac{\ln(1-\hat{\tau})}{1-\hat{\tau}}\right)_+ - 2\frac{1+\hat{\tau}^2}{1-\hat{\tau}}\ln\hat{\tau}\right\}$$

Note: $[\cdots]_+$ is a distribution,

$$\int_0^1 dz\, f(z)\left[\frac{1}{1-z}\right]_+ = \int_0^1 dz\frac{f(z)-f(1)}{1-z},$$ which is finite.

- In the soft limit, $\hat{\tau}\to 1$ $\left(\hat{\tau}=\frac{M^2}{\hat{s}}\right)$,

$$\sigma^{(1)}_{\text{real}}\left(q\overline{q}'\right) \longrightarrow \sigma^{(0)}\frac{\alpha_s}{2\pi}\left(\frac{4\pi\mu^2}{M^2}\right)^{\varepsilon}\frac{\Gamma(1-\varepsilon)}{\Gamma(1-2\varepsilon)}\cdot C_F$$
$$\cdot\left\{\frac{2}{\varepsilon^2}\delta(1-\hat{\tau}) - \frac{4}{\varepsilon}\frac{1}{(1-\hat{\tau})_+} + 8\left(\frac{\ln(1-\hat{\tau})}{1-\hat{\tau}}\right)_+\right\}$$

$\left(q\bar{q}'\right)_{virt} + \left(q\bar{q}'\right)_{\text{real}}$ at NLO

- $$\sigma^{(1)}_{q\bar{q}'} = \sigma^{(1)}_{virt}\left(q\bar{q}'\right) + \sigma^{(1)}_{\text{real}}\left(q\bar{q}'\right)$$
$$= \sigma^{(0)}\frac{\alpha_s}{2\pi}\left(\frac{4\pi\mu^2}{M^2}\right)^{\varepsilon}\frac{\Gamma\left(1-\varepsilon\right)}{\Gamma\left(1-2\varepsilon\right)}\cdot C_F$$
$$\cdot\left\{\frac{-2}{\varepsilon}\left(\frac{1+\hat{\tau}^2}{1-\hat{\tau}}\right)_+ - 2\frac{1+\hat{\tau}^2}{1-\hat{\tau}}\ln\hat{\tau} + 4\left(1+\hat{\tau}^2\right)\left(\frac{\ln\left(1-\hat{\tau}\right)}{1-\hat{\tau}}\right)_+\right.$$
$$\left. + \left(\frac{2\pi^2}{3} - 8\right)\delta\left(1-\hat{\tau}\right)\right\}$$

  Where we have used
$$\frac{-2}{\varepsilon}\left[\frac{1+\hat{\tau}^2}{\left(1-\hat{\tau}\right)_+} + \frac{3}{2}\delta\left(1-\hat{\tau}\right)\right] = \frac{-2}{\varepsilon}\left(\frac{1+\hat{\tau}^2}{1-\hat{\tau}}\right)_+$$

- All the soft singularities $\left(\frac{1}{\varepsilon^2}, \frac{1}{\varepsilon}\right)$ cancel in $\sigma^{(1)}_{q\bar{q}'}$

  $\Rightarrow$ KLN theorem

  (Kinoshita-Lee-Navenberg)

- $$\sigma^{(1)}_{q\bar{q}'} \sim \frac{1}{\varepsilon}(\text{term}) + \text{finite (terms)}$$

  ↑

  Collinear Singularity

Factorization Theorem

- Perturbative PDF

$\phi^{(0)}_{i/k} = \delta_{ik}\delta(1-x)$

$\frac{\alpha_s}{\pi}\phi^{(1)}_{i/k}$ can be calculated from the definition of PDF.

(Process independent,but factorization scheme dependent)

- (1)

$$\sigma^{(0)}_{kl} =$$

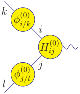

$$\Rightarrow H^{(0)}_{kl} = \sigma^{(0)}_{kl}$$

(2)

$$\sigma^{(1)}_{kl} =$$

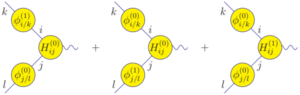

Factorization scheme dependent

$$\Rightarrow H^{(1)}_{kl} = \sigma^{(1)}_{kl} - \left[\phi^{(1)}_{i/k} H^{(0)}_{il} + H^{(0)}_{kj}\phi^{(1)}_{j/l}\right]$$

Finite   Divergent

Perturbative PDF

- In $\overline{MS}$-scheme (modified minimal subtraction)

$$\phi^{(1)}_{q/q}(z) = \phi^{(1)}_{\bar{q}/\bar{q}}(z) = \frac{-1}{\varepsilon}\frac{1}{2}\left(4\pi e^{-\gamma_E}\right)^{\varepsilon} P^{(1)}_{q\leftarrow q}(z)$$
$$\phi^{(1)}_{q/g}(z) = \phi^{(1)}_{\bar{q}/g}(z) = \frac{-1}{\varepsilon}\frac{1}{2}\left(4\pi e^{-\gamma_E}\right)^{\varepsilon} P^{(1)}_{q\leftarrow g}(z)$$

where the splitting kernel for 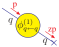

is

$$P^{(1)}_{q\leftarrow q}(z) = C_F\left(\frac{1+z^2}{1-z}\right)_+$$
$$= C_F\left(\frac{1+z^2}{(1-z)_+} + \frac{3}{2}\delta(1-z)\right),$$

and for 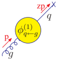

is

$$P^{(1)}_{q\leftarrow g}(z) = T_R\left(z^2 + (1-z)^2\right),$$

where $C_F = \frac{4}{3}$ and $T_R = \frac{1}{2}$.

Note: The Pole part in the $\overline{MS}$ scheme is

$$\frac{1}{\hat{\varepsilon}} = \frac{1}{\varepsilon}(4\pi e^{-\gamma_E})^{\varepsilon} = \frac{1}{\varepsilon} + \ln 4\pi - \gamma_E$$

In the MS scheme, the pole part is just $\frac{1}{\varepsilon}$

Find $H^{(1)}_{q\bar{q}'}$ (in the $\overline{MS}$ scheme)

- Take off the factor $\left(\frac{\alpha_s}{\pi}\right)$

$$\sigma^{(1)}_{q\bar{q}'} = \sigma^{(0)}\left\{P^{(1)}_{q\leftarrow q}(\hat{\tau})\left[\ln\left(\frac{M^2}{\mu^2}\right) - \frac{1}{\varepsilon} + \gamma_E - \ln 4\pi\right]\right.$$
$$\left. +C_F\left[-\frac{1+\hat{\tau}^2}{1-\hat{\tau}}\ln\hat{\tau} + 2\left(1+\tau^2\right)\left(\frac{\ln(1-\hat{\tau})}{1-\hat{\tau}}\right)_+ + \left(\frac{\pi^2}{3} - 4\right)\delta(1-\hat{\tau})\right]\right\}$$

-

$$H^{(1)}_{q\bar{q}'}(\hat{\tau}) = \sigma^{(1)}_{q\bar{q}'} - \left[2\phi^{(1)}_{q\leftarrow q}\sigma^{(0)}_{q\bar{q}'}\right]$$
$$= \hat{\sigma}^{(0)}\cdot\left\{P^{(1)}_{q\leftarrow q}(\hat{\tau})\ln\left(\frac{M^2}{\mu^2}\right)\right.$$
$$\left. +C_F\left[-\frac{1+\hat{\tau}^2}{1-\hat{\tau}}\ln\hat{\tau} + 2\left(1+\tau^2\right)\left(\frac{\ln(1-\hat{\tau})}{1-\hat{\tau}}\right)_+ + \left(\frac{\pi^2}{3} - 4\right)\delta(1-\hat{\tau})\right]\right\}$$

where

$$\hat{\tau} = \frac{M^2}{\hat{s}} = \frac{M^2}{x_1x_2S}, \qquad \sigma^{(0)} = \hat{\sigma}^{(0)}\cdot(1-\varepsilon),$$
$$\hat{\sigma}^{(0)} = \frac{\pi}{12\hat{s}}g_w^2 = \frac{\pi g_w^2}{12S}\frac{1}{x_1x_2}.$$

- pQCD prediction

$$\sigma_{hh'} = \left\{\sum_{f=q,\bar{q}'}\int dx_1dx_2\phi_{f/h}\left(x_1,\mu^2\right)\left[\sigma^{(0)}\delta(1-\hat{\tau})\right]\phi_{\bar{f}/h'}\left(x_2,\mu^2\right)\right.$$
$$+\sum_{f=q,\bar{q}'}\int dx_1dx_2\phi_{f/h}\left(x_1,\mu^2\right)\left[\frac{\alpha_s\left(\mu^2\right)}{\pi}H^{(1)}_{f\bar{f}}(\hat{\tau})\right]\phi_{\bar{f}/h'}\left(x_2,\mu^2\right)$$
$$\left.+\sum_{f=q,\bar{q}'}\int dx_1dx_2\phi_{f/h}\left(x_1,\mu^2\right)\left[\frac{\alpha_s\left(\mu^2\right)}{\pi}H^{(1)}_{fG}(\hat{\tau})\right]\phi_{G/h'}\left(x_2,\mu^2\right) + (x_1\leftrightarrow x_2)\right\}$$

"Renormalization" and "Factorization"

	UV renormalization		Collinear/soft factorization	
A:	Bare Green Func.	$G_0(\alpha_0, m_0, ..)$	Partonic X-sect	F_a
B:	Ren. constants	$Z_i(\mu)$	Pert. parton dist.	$f_a^b(\mu)$
C:	Ren. Green Fun.	$G_R = G_0/Z$	Hard X-sect	$\hat{F} = F\,/\,f$
D:	Anomalous dim.	$\gamma = \frac{\mu}{Z}\frac{d}{d\mu}Z$	Splitting fun.	$P = \frac{\mu}{f}\frac{d}{d\mu}f$
E:	Phys. para. α, m	$\alpha_0 Z_i \ldots$	Had. parton dist. f_A	resummed
F:	Phys sc. amp.	$\alpha(\mu)\, G_R(m, \mu)$	Hadronic S.F.'s F_A	$f_A(\mu) \times \hat{F}(\mu)$

Some common features:

A : divergent; but, independent of "scheme" and scale μ;

B : divergent; scale and scheme dependent;
universal; absorbs all ultra-violet/soft/collinear divergences;

C & D : finite; scheme-dependent;
D controls the μ dependence of E & F;

E : physical parameters to be obtained from experiment;

F : Theoretical "prediction"; μ-indep. to all orders,
but μ-dep. at finite order n; $\mu\frac{d}{d\mu} \sim \mathcal{O}(\alpha^{n+1})$

Note: "Renormalization" is factorization (of UV divergences);
"factorization" is renormalization (of soft/collinear div.)

QCD factorization and PDFs

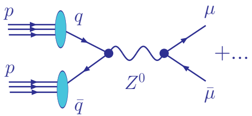

According to QCD factorization theorems, typical cross sections (e.g., for $p(k_1)p(k_2) \to \left[Z(q) \to \ell(k_3)\bar{\ell}(k_4)\right] X$) take the form

$$\sigma_{pp\to\ell\bar{\ell}X} = \sum_{a,b=q,\bar{q},g} \int_0^1 d\xi_1 \int_0^1 d\xi_2\, \widehat{\sigma}_{ab\to Z\to\ell\bar{\ell}}\left(\frac{x_1}{\xi_1}, \frac{x_2}{\xi_2}; \frac{Q}{\mu}\right) f_{a/p}(\xi_1,\mu) f_{b/p}(\xi_2,\mu) + \mathcal{O}\left(\Lambda^2_{QCD}/Q^2\right)$$

Once we computed **partonic** cross sections $\widehat{\sigma}_{ab\to(Z\to\ell\bar{\ell})X}$, we must convolve them with proton PDFs $f_{a/p}(\xi_1,\mu)$ and $f_{b/p}(\xi_2,\mu)$.

Operator definitions for PDFs

To all orders in α_s, PDFs are **defined** as matrix elements of certain correlator functions:

$$f_{q/p}(x,\mu) = \frac{1}{4\pi}\int_{-\infty}^{\infty} dy^- e^{iy^- p^+} \langle p \left| \overline{\psi}_q(0, y^-, \vec{0}_T)\gamma^+ \psi_q(0,0,\vec{0}_T) \right| p \rangle, \text{ etc.}$$

The exact form of $f_{a/p}$ is not known; but its μ dependence is described by **D**okshitzer-**G**ribov-**L**ipatov-**A**ltarelli-**P**arisi (**DGLAP**) equations:

$$\mu \frac{df_{i/p}(x,\mu)}{d\mu} = \sum_{j=g,u,\bar{u},d,\bar{d},\ldots} \int_x^1 \frac{dy}{y} P_{i/j}\left(\frac{x}{y}, \alpha_s(\mu)\right) f_{j/p}(y,\mu)$$

$P_{i/j}$ are probabilities for $j \to ik$ collinear splittings;
are known to order α_s^3 (NNLO):

$$P_{i/j}(x,\alpha_s) = \alpha_s P_{i/j}^{(1)}(x) + \alpha_s^2 P_{i/j}^{(2)}(x) + \alpha_s^3 P_{i/j}^{(3)}(x) + \ldots$$

Universality of PDFs

To all orders in α_s, PDFs are **defined** as matrix elements of certain correlator functions:

$$f_{q/p}(x,\mu) = \frac{1}{4\pi}\int_{-\infty}^{\infty} dy^- e^{iy^- p^+} \langle p \left| \overline{\psi}_q(0,y^-,\vec{0}_T)\gamma^+\psi_q(0,0,\vec{0}_T) \right| p\rangle, \text{ etc.}$$

PDFs are **universal** – depend only on the type of the hadron (p) and parton (q, $\bar{q}$, g)

... can be **parametrized** as

$$f_{i/p}(x,Q_0) = a_0 x^{a_1}(1-x)^{a_2} F(a_3,a_4,...) \text{ at } Q_0 \sim 1 \text{ GeV}$$

... predicted by solving DGLAP equations at $\mu > Q_0$

Example of DGLAP evolution

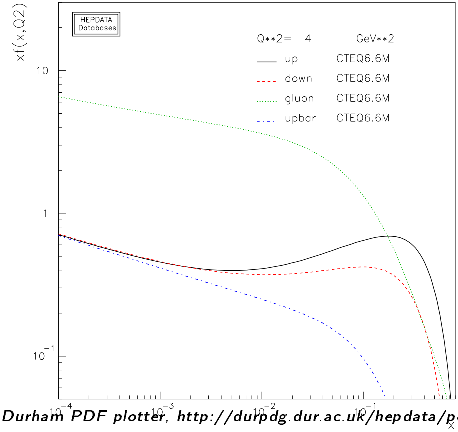

Durham PDF plotter, http://durpdg.dur.ac.uk/hepdata/pdf3.html

Compare μ dependence of u quark PDF and the gluon PDF

The u, d PDFs have a characteristic bump at $x \sim 1/3$ – reminiscent of early valence quark models of the proton structure

The PDFs rise rapidly at $x < 0.1$ as a consequence of perturbative evolution

Example of DGLAP evolution

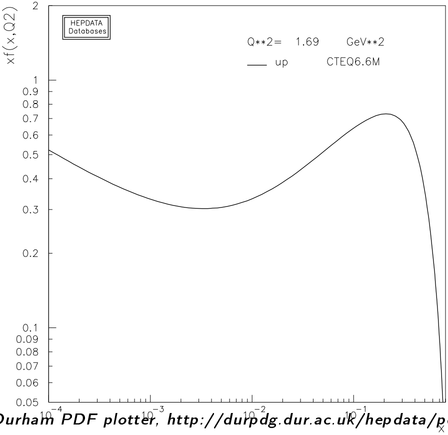

Durham PDF plotter, http://durpdg.dur.ac.uk/hepdata/pdf3.html

As Q increases, it becomes more likely that a high-x parton loses some momentum through QCD radiation

$\Rightarrow u(x,Q)$ reduces at $x \gtrsim 0.1$, increases at $x \lesssim 0.1$

Example of DGLAP evolution

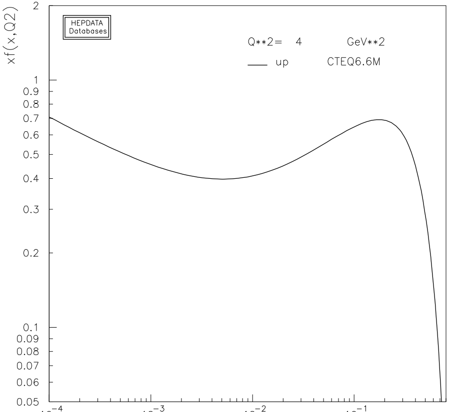

Durham PDF plotter, http://durpdg.dur.ac.uk/hepdata/pdf3.html

As Q increases, it becomes more likely that a high-x parton loses some momentum through QCD radiation

$\Rightarrow u(x,Q)$ reduces at $x \gtrsim 0.1$, increases at $x \lesssim 0.1$

Example of DGLAP evolution

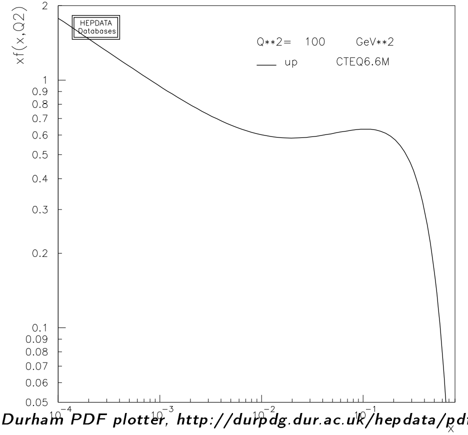

Durham PDF plotter, http://durpdg.dur.ac.uk/hepdata/pdf3.html

As Q increases, it becomes more likely that a high-x parton loses some momentum through QCD radiation

$\Rightarrow u(x, Q)$ reduces at $x \gtrsim 0.1$, increases at $x \lesssim 0.1$

Example of DGLAP evolution

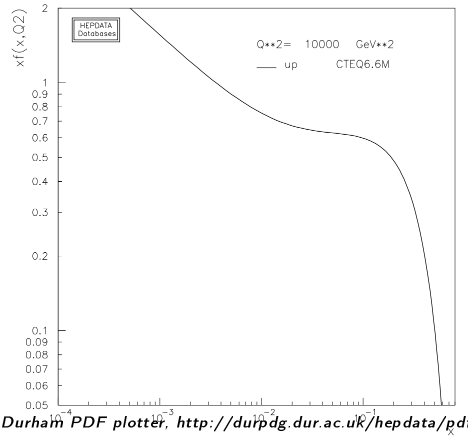

Durham PDF plotter, http://durpdg.dur.ac.uk/hepdata/pdf3.html

As Q increases, it becomes more likely that a high-x parton loses some momentum through QCD radiation

$\Rightarrow u(x,Q)$ reduces at $x \gtrsim 0.1$, increases at $x \lesssim 0.1$

Example of DGLAP evolution: $\bar{u}$ and gluon PDF

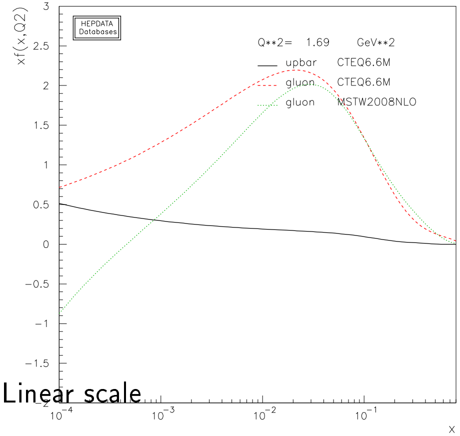

$g(x, Q)$ can become negative at $x < 10^{-2}$, $Q < 2$ GeV

may lead to unphysical predictions

This is an indication that DGLAP factorization experiences difficulties at such small x and Q

Large $\ln^k(1/x)$ in $P_{i/j}(x)$ break PQCD expansion at $x \sim Q/\sqrt{s} \ll 1$

Example of DGLAP evolution: $\bar{u}$ and gluon PDF

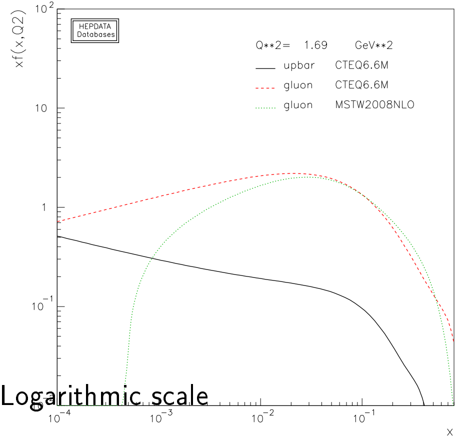

Logarithmic scale

$g(x, Q)$ can become negative at $x < 10^{-2}$, $Q < 2$ GeV

may lead to unphysical predictions

This is an indication that DGLAP factorization experiences difficulties at such small x and Q

Large $\ln^k(1/x)$ in $P_{i/j}(x)$ break PQCD expansion at $x \sim Q/\sqrt{s} \ll 1$

Example of DGLAP evolution: $\bar{u}$ and gluon PDF

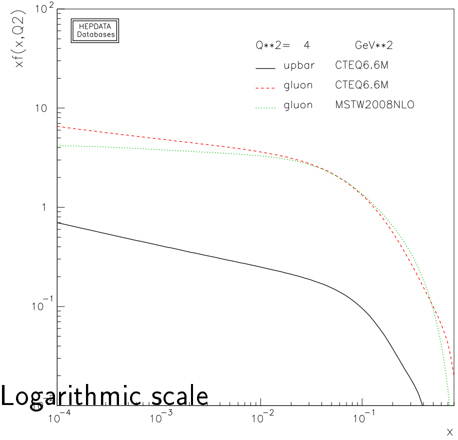

Logarithmic scale

As Q increases, $g(x, Q)$ grows rapidly at small x

$\alpha_s(Q)$ becomes small enough to suppress $\ln^k(1/x)$ terms

small-x behavior stabilizes

Example of DGLAP evolution: $\bar{u}$ and gluon PDF

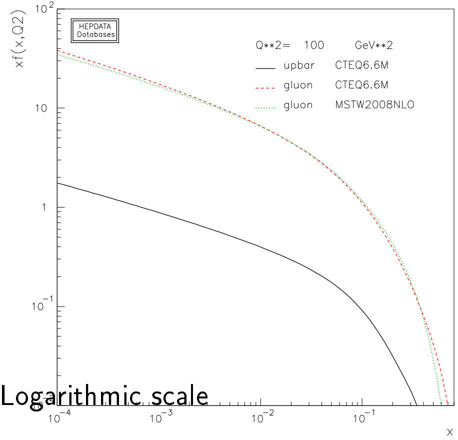

Logarithmic scale

As Q increases, $g(x,Q)$ grows rapidly at small x

$\alpha_s(Q)$ becomes small enough to suppress $\ln^k(1/x)$ terms

small-x behavior stabilizes

Example of DGLAP evolution: $\bar{u}$ and gluon PDF

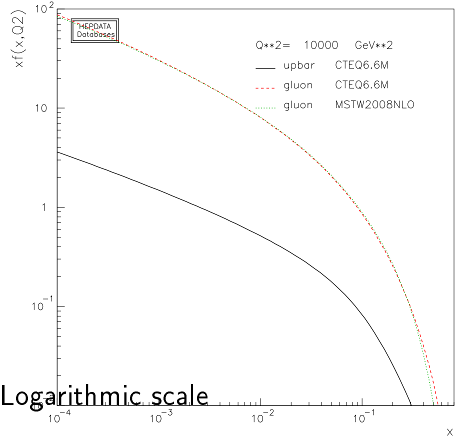

Logarithmic scale

As Q increases, $g(x,Q)$ grows rapidly at small x

$\alpha_s(Q)$ becomes small enough to suppress $\ln^k(1/x)$ terms

small-x behavior stabilizes

Where do the PDFs come from?

Where do the PDFs come from?

- From a combination of BIG, medium, and **small** experiments
- Complementarity in
  - kinematical ranges
  - systematics

+ lattice QCD

LHC
Tevatron

HERA
RHIC
EIC

Fixed-target experiments

Recent CT10 NNLO PDFs

[arXiv:1302.6246]

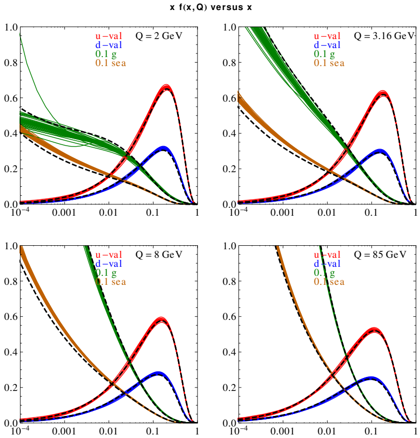

FIG. 2: CT10NNLO parton distribution functions. These figures show the Hessian error PDFs from the CT10NNLO analysis. Each graph shows $x\,u_{\text{valence}} = x(u-\overline{u}), x\,d_{\text{valence}} = x(d-\overline{d}), 0.10\,x\,g$ and $0.10\,x\,q_{\text{sea}}$ as functions of x for a fixed value of Q. The values of Q are 2, 3.16, 8, 85 GeV. The quark sea contribution is $q_{\text{sea}} = 2(\overline{d}+\overline{u}+\overline{s})$. The dashed curves are the central CT10 NLO fit.

CT10 NNLO describes well LHC 7 TeV experiments

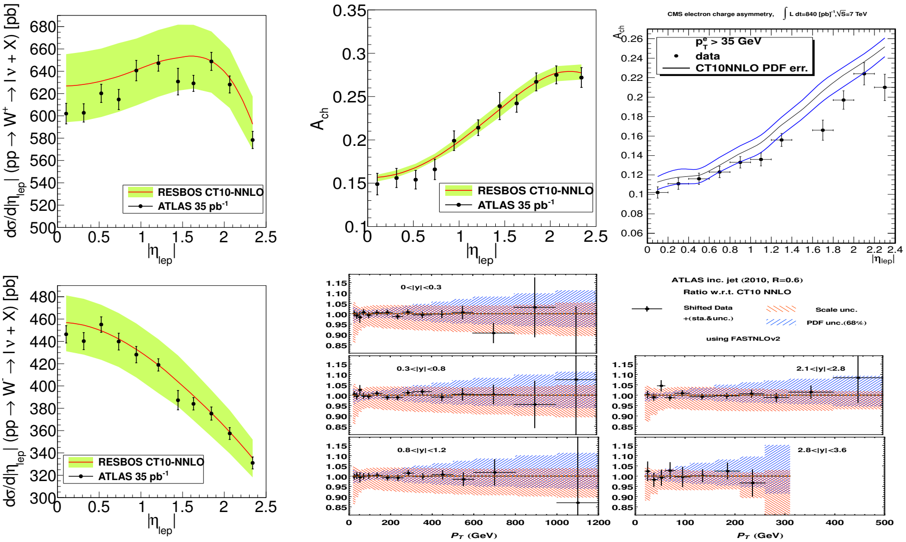

NNLO gluon PDF $xg(x, Q)$ from 5 groups

Linear x scale

Logarithmic x scale

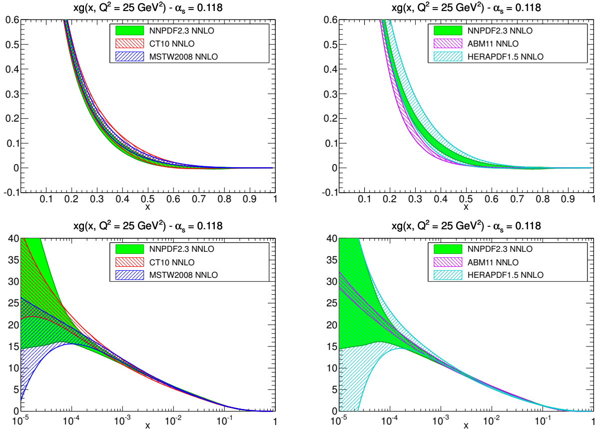

R. Ball, et al., 1211.5142

Several PDF groups provide their parametrizations of PDFs. How are these parametrizations obtained?

The flow of the PDF analysis

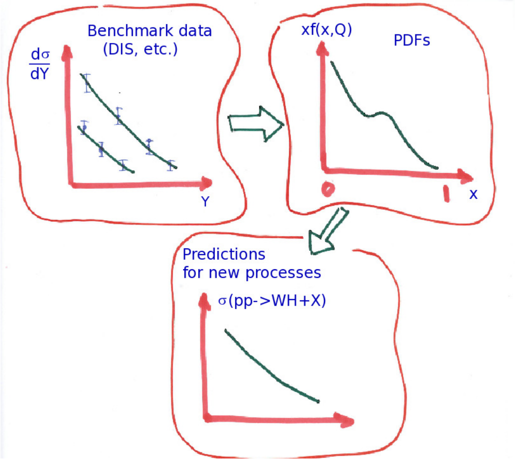

PDFs are not measured directly, but some data sets are sensitive to specific combinations of PDFs. By constraining these combinations, the PDFs can be disentangled in a combined (global) fit.

The flow of the PDF analysis

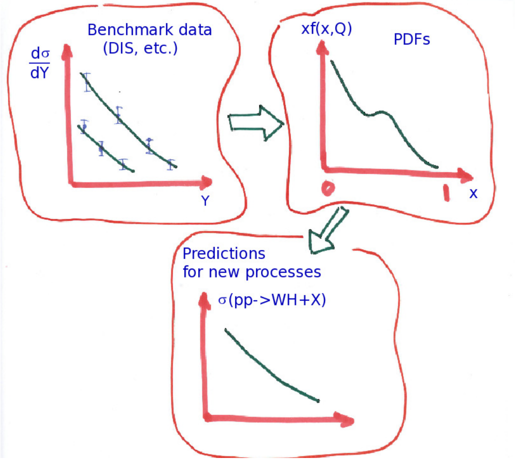

Data sets and $\chi^2/d.o.f.$ in CT10 NNLO and CT10W NLO analyses

Experimental data set	N_{pt}	CT10NNLO	CT10W
Combined HERA1 NC and CC DIS [74]	579	1.07	1.17
BCDMS F_2^p [75]	339	1.16	1.14
BCDMS F_2^d [76]	251	1.16	1.12
NMC F_2^p [77]	201	1.66	1.71
NMC F_2^d/F_2^p [77]	123	1.23	1.28
CDHSW F_2^p [78]	85	0.83	0.66
CDHSW F_3^p [78]	96	0.81	0.75
CCFR F_2^p [79]	69	0.98	1.02
CCFR xF_3^p [80]	86	0.40	0.59
NuTeV neutrino dimuon SIDIS [81]	38	0.78	0.94
NuTeV antineutrino dimuon SIDIS [81]	33	0.86	0.91
CCFR neutrino dimuon SIDIS [82]	40	1.20	1.25
CCFR antineutrino dimuon SIDIS [82]	38	0.70	0.78
H1 F_2^c [83]	8	1.17	1.26
H1 σ_r^c for $c\bar{c}$ [59, 84]	10	1.63	1.54
ZEUS F_2^c [57]	18	0.74	0.90
ZEUS F_2^c [58]	27	0.62	0.76
E605 Drell-Yan process, $\sigma(pA)$ [85]	119	0.80	0.81
E866 Drell Yan process, $\sigma(pd)/(2\sigma(pp))$ [86]	15	0.65	0.64
E866 Drell-Yan process, $\sigma(pp)$ [87]	184	1.27	1.21
CDF Run-1 W charge asymmetry [88]	11	1.22	1.24
CDF Run-2 W charge asymmetry [89]	11	1.04	1.02
DØ Run-2 $W \to e\nu_e$ charge asymmetry [90]	12	2.17	2.11
DØ Run-2 $W \to \mu\nu_\mu$ charge asymmetry [91]	9	1.65	1.49
DØ Run-2 Z rapidity distribution [92]	28	0.56	0.54
CDF Run-2 Z rapidity distribution [93]	29	1.60	1.44
CDF Run-2 inclusive jet production [94]	72	1.42	1.55
DØ Run-2 inclusive jet production [95]	110	1.04	1.13
Total	**2641**	**1.11**	**1.13**

Modern fits involve up to 40 experiments, 5000+ data points, and 100+ free parameters

The flow of the PDF analysis

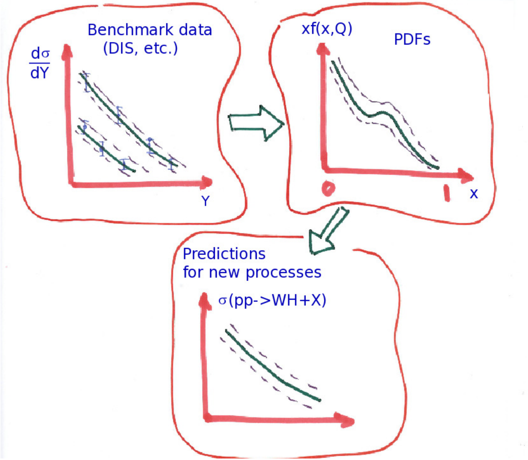

We are interested not just in one best fit, but also in the uncertainty of the resulting PDF parametrizations and theoretical predictions based on them.

Stages of the PDF analysis

1. Select valid experimental data
2. Assemble most precise theoretical cross sections and verify their mutual consistency
3. Choose the functional form for PDF parametrizations
4. Implement a procedure to handle nuisance parameters (>200 sources of correlated experimental errors)
5. Perform a fit
6. Make the new PDFs and their uncertainties available to end users

Requirements for PDF parametrizations

PDF parametrizations for $f_{a/p}(x,Q)$ must be "flexible just enough" to reach agreement with the data, without violating QCD constraints (sum rules, positivity, ...) or reproducing random fluctuations

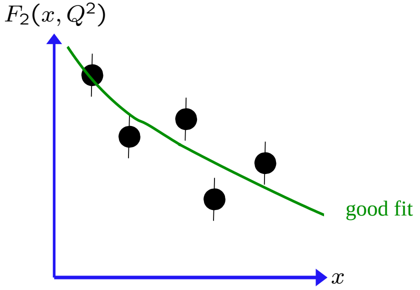

Requirements for PDF parametrizations

PDF parametrizations for $f_{a/p}(x, Q)$ must be "flexible just enough" to reach agreement with the data, without violating QCD constraints (sum rules, positivity, ...) or reproducing random fluctuations

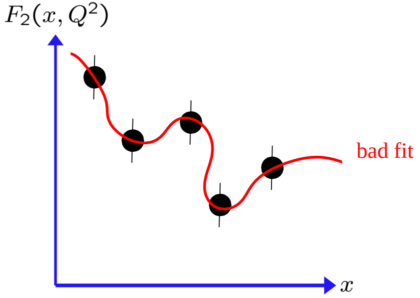

Requirements for PDF parametrizations

PDF parametrizations for $f_{a/p}(x, Q)$ must be "flexible just enough" to reach agreement with the data, without violating QCD constraints (sum rules, positivity, ...) or reproducing random fluctuations

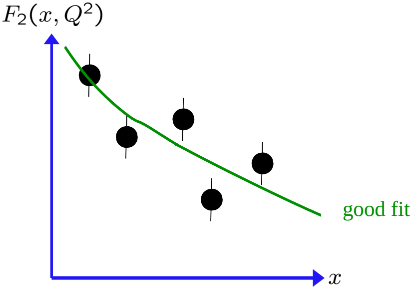

Traditional solution

"Theoretically motivated" functions with a few parameters

$$f_{i/p}(x, Q_0) = a_0 x^{a_1} (1 - x)^{a_2} \times F(x; a_3, a_4, ...)$$

- $x \to 0$: $f \propto x^{a_1}$ – Regge-like behavior
- $x \to 1$: $f \propto (1 - x)^{a_2}$ – quark counting rules
- $F(a_3, a_4, ...)$ affects intermediate x; just a convenient functional form

Requirements for PDF parametrizations

PDF parametrizations for $f_{a/p}(x,Q)$ must be "flexible just enough" to reach agreement with the data, without violating QCD constraints (sum rules, positivity, ...) or reproducing random fluctuations

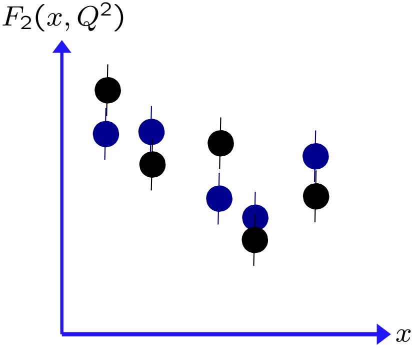

Radical solution

Neural Network PDF collaboration

- Generate N replicas of the experimental data, randomly scattered around the original data in accordance with the probability suggested by the experimental errors
- Divide the replicas into a fitting sample and control sample

Requirements for PDF parametrizations

PDF parametrizations for $f_{a/p}(x, Q)$ must be "flexible just enough" to reach agreement with the data, without violating QCD constraints (sum rules, positivity, ...) or reproducing random fluctuations

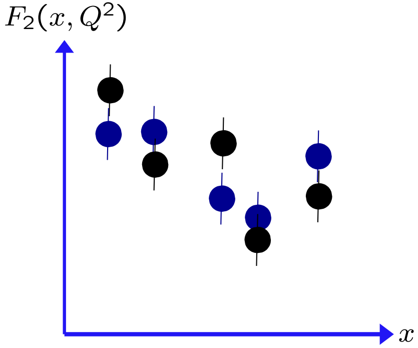

Radical solution

Neural Network PDF collaboration

- Parametrize $f_{a/p}(x, Q)$ by ultra-flexible functions — neural networks
- A statistical theorem states that any function can be approximated by a neural network with a sufficient number of nodes (in practice, of order 10)

Requirements for PDF parametrizations

PDF parametrizations for $f_{a/p}(x,Q)$ must be "flexible just enough" to reach agreement with the data, without violating QCD constraints (sum rules, positivity, ...) or reproducing random fluctuations

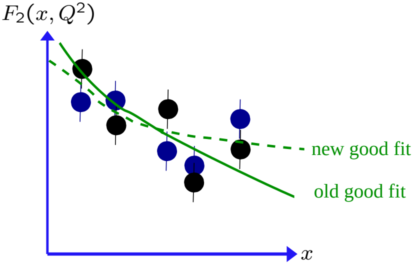

Radical solution

Neural Network PDF collaboration

- Fit the neural nets to the fitting sample, while demanding good agreement with the control sample
- Smoothness of $f_{a/p}(x,Q)$ is preserved, despite its nominal flexibility

Hessian error PDFs (CT10)

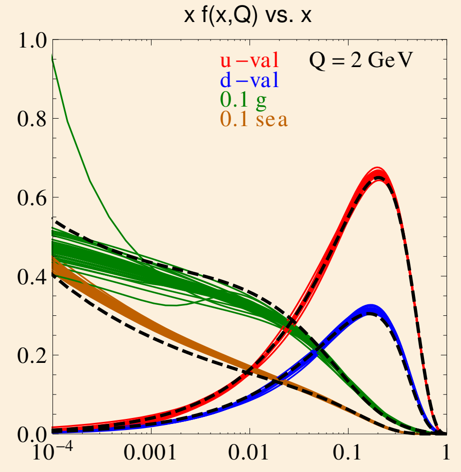

Neural network PDFs

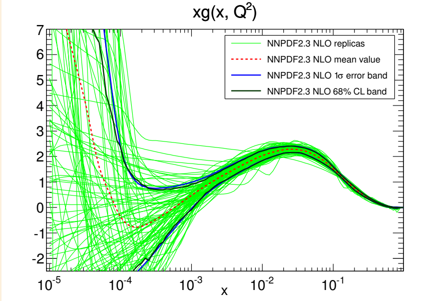

Multi-dimensional error analysis

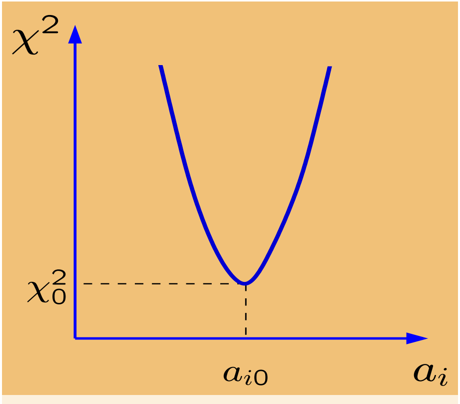

- Minimization of a likelihood function (χ^2) with respect to ~ 30 theoretical (mostly PDF) parameters $\{a_i\}$ and > 100 experimental systematical parameters

Multi-dimensional error analysis

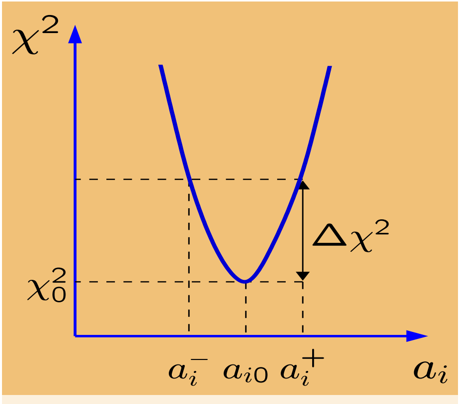

- Establish a confidence region for $\{a_i\}$ for a given tolerated increase in χ^2
- In the ideal case of perfectly compatible Gaussian errors, 68% c.l. on a physical observable X corresponds to $\Delta\chi^2 = 1$ independently of the number N of PDF parameters

See, e.g., P. Bevington, K. Robinson, Data analysis and error reduction for the physical sciences

Multi-dimensional error analysis

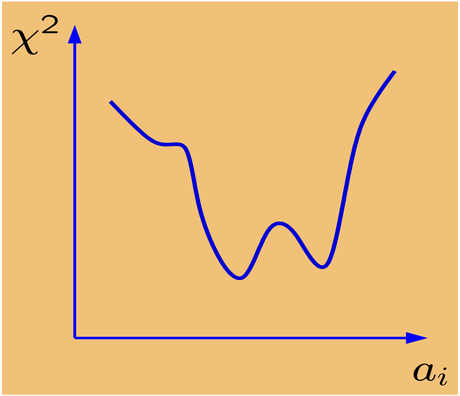

Pitfalls to avoid

- "Landscape"
  - disagreements between the experiments

In the worst situation, significant disagreements between M experimental data sets can produce up to $N \sim M!$ possible solutions for PDF's, with $N \sim 10^{500}$ reached for "only" about 200 data sets

Multi-dimensional error analysis

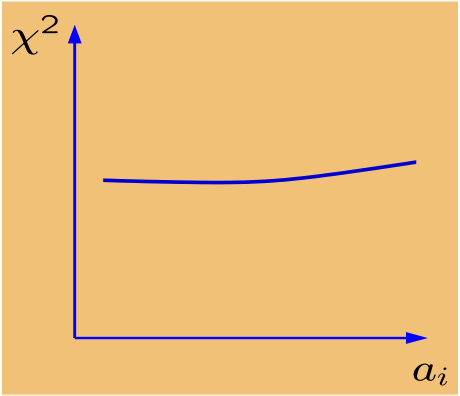

Pitfalls to avoid

- Flat directions
  - unconstrained combinations of PDF parameters
  - dependence on free theoretical parameters, especially in the PDF parametrization
  - impossible to derive reliable PDF error sets

Multi-dimensional error analysis

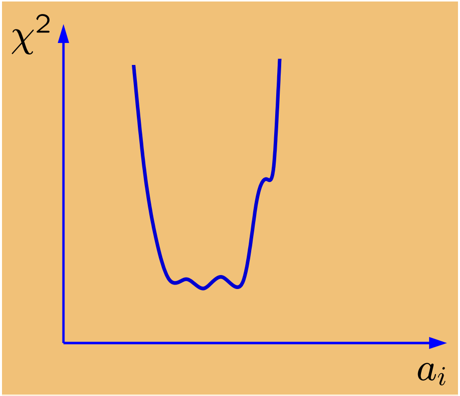

The actual χ^2 function shows

- a well pronounced global minimum χ_0^2
- weak tensions between data sets in the vicinity of χ_0^2 (mini-landscape)
- some dependence on assumptions about flat directions

Multi-dimensional error analysis

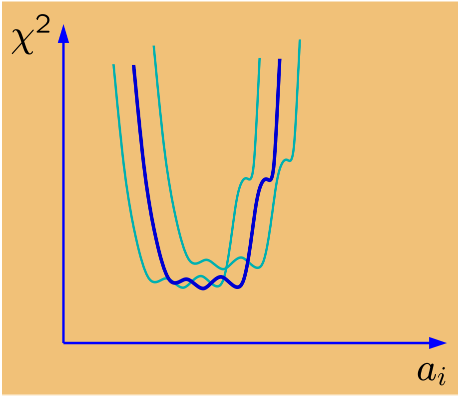

The actual χ^2 function shows

- a well pronounced global minimum χ_0^2
- weak tensions between data sets in the vicinity of χ_0^2 (mini-landscape)
- some dependence on assumptions about flat directions

Multi-dimensional error analysis

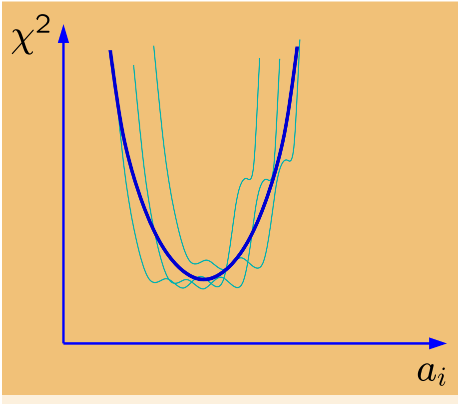

The actual χ^2 function shows

- a well pronounced global minimum χ_0^2
- weak tensions between data sets in the vicinity of χ_0^2 (mini-landscape)
- some dependence on assumptions about flat directions

The likelihood is approximately described by a quadratic χ^2 with a revised tolerance condition $\Delta\chi^2 \leq T^2$

Multi-dimensional error analysis

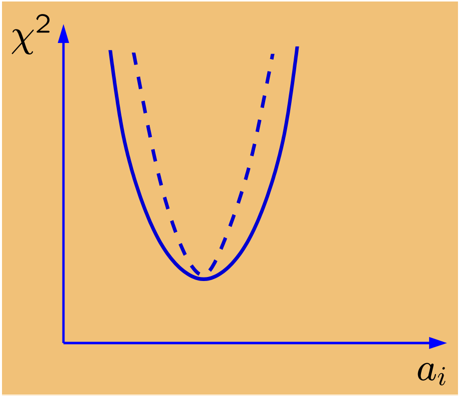

The actual χ^2 function shows

- a well pronounced global minimum χ_0^2
- weak tensions between data sets in the vicinity of χ_0^2 (mini-landscape)
- some dependence on assumptions about flat directions

The likelihood is approximately described by a quadratic χ^2 with a revised tolerance condition $\Delta\chi^2 \leq T^2$

Multi-dimensional error analysis

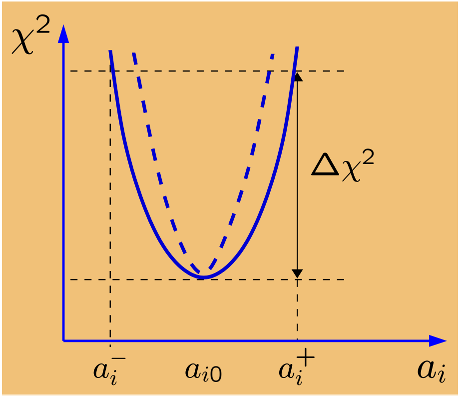

The actual χ^2 function shows

- a well pronounced global minimum χ_0^2
- weak tensions between data sets in the vicinity of χ_0^2 (mini-landscape)
- some dependence on assumptions about flat directions

The likelihood is approximately described by a quadratic χ^2 with a revised tolerance condition $\Delta\chi^2 \le T^2$

Confidence intervals in global PDF analyses

Monte-Carlo sampling of the PDF parameter space

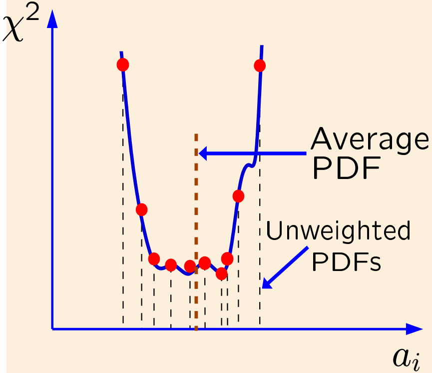

A very general approach that

- realizes stochastic sampling of the probability distribution

(Alekhin; Giele, Keller, Kosower; NNPDF)

- can parametrize PDF's by flexible neural networks (NNPDF)
- does not rely on smoothness of χ^2 or Gaussian approximations

Modern parton distribution functions

...are indispensable in computations of inclusive hadronic reactions at CERN and other laboratories

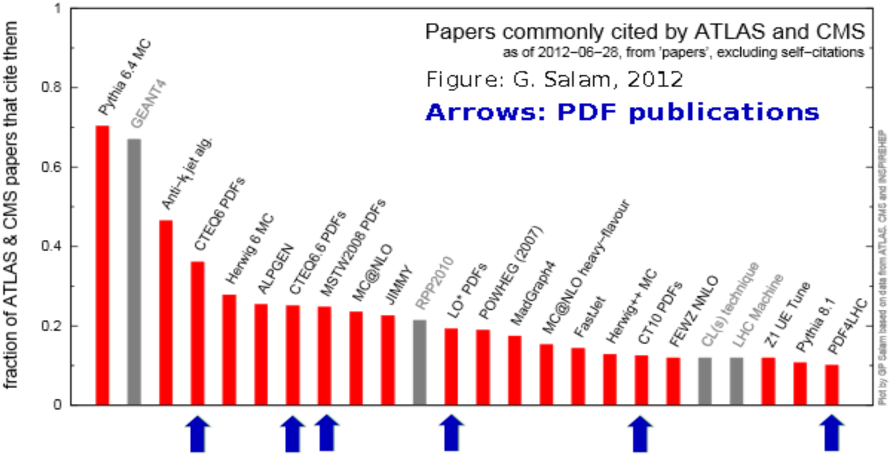

Conclusions

- QCD theory **at all energies** undergoes rapid developments, with much attention paid to
  - ingenious **perturbative** computations for multi-particle states, fully differential cross sections
  - new **factorization** methods for differential cross sections and all-order **resummations**
  - sophisticated analysis of **nonperturbative** hadronic functions
- The global analysis help us to understand rich interconnections between perturbative and nonperturbative features of QCD processes and make sense of rich LHC dynamics